Biogeosciences, 7, 371–386, 2010
www.biogeosciences.net/7/371/2010/

Biogeosciences

Interannual variability of alongshore spring bloom dynamics in a coastal sea caused by the differential influence of hydrodynamics and light climate

G. Brandt[1,*] **and K. W. Wirtz**[1]

[1]GKSS-Research Centre, Institute for Coastal Research, Max-Planck-Str. 1, 21502 Geesthacht, Germany
[*]currently at: Bundesamt für Seeschifffahrt und Hydrographie, Bernhard-Nocht-Str. 78, 20359 Hamburg, Germany

Received: 26 April 2009 – Published in Biogeosciences Discuss.: 13 May 2009
Revised: 8 December 2009 – Accepted: 10 January 2010 – Published: 29 January 2010

Abstract. Timing and spatial distribution of phytoplankton blooms in coastal oceans are highly variable. The interactions of various biological and physical factors leading to the observed variability are complex and remain poorly understood. We present an example for distinct differences in the spatio-temporal chlorophyll *a* (CHL-*a*) distribution on an interannual scale, integrating high-frequency data from an autonomous measuring device (FerryBox), which operated on an alongshore route in the coastal German Bight (North Sea). While in one year the distribution of CHL-*a* was spatially homogeneous (2004), a bloom only developed in one part of the transect in the following spring period (2005). We use a one-dimensional Lagrangian particle tracking model, which operates along the mean current direction, combined with a NPZ-model to identify the mechanisms controlling the observed interannual bloom variability on the alongshore transect. Our results clearly indicate that in 2004 the local light climate determined the spatial and temporal dynamics of the spring bloom. In contrast, the import of a water mass with elevated CHL-*a* concentrations from the adjacent Southern Bight triggered the spring bloom in 2005. The inflow event did, however, not last long enough to spread the bloom into the eastern part of the study area, where high turbidity prevented local phytoplankton growth. The model identifies two interacting mechanisms, light climate and hydrodynamics, that controlled the alongshore dynamics. Especially the occurrence of a pronounced spring bloom despite unfavourable light conditions in 2005 underlines the need to carefully consider hydrodynamics to understand the dynamics of the plankton community in coastal environments.

Correspondence to: G. Brandt
(brandt@bpt-info.de)

1 Introduction

The phytoplankton spring bloom drives food web dynamics and matter cycling in most temperate aquatic ecosystems (Sommer, 1998). Despite its recurrence, timing, spatial extent, and duration of the first seasonal peak in algal concentration show considerable interannual variation. While in deep waters the onset of a bloom typically follows stratification in spring, interannual variability and spatial heterogeneity are particularly strong in shallow coastal seas (Thomas et al., 2003; Cloern, 1996). Only the magnitude of the bloom seems to be predictable as a function of winter nutrient concentration (Loebl et al., 2009; Muylaert et al., 2006; Cloern, 1996). Before and during the bloom event, however, the balance between algal production and loss in near-shore waters is sensitive to a multitude of different factors such as temperature, water transparency, abundance of herbivores, stratification, or incident irradiance. While a change in light availability is often triggering the spring bloom (Tian et al., 2009; Townsend et al., 1994), grazing by zooplankton or benthic filter feeders is typically the main cause for the breakdown of a bloom (Irigoien et al., 2005; Greve et al., 2004). Hence, the observed variability mainly reflects the sensitivity of the spring bloom development to fluctuating physical and biological conditions.

Particularly in the coastal ocean, wind- or tide-generated turbulence critically affects the development of phytoplankton in spring. Strong turbulence, leading to vertical mixing, counteracts water column stratification and retards algal growth. It also decreases light availability for phytoplankton by increasing turbidity, which is suggested to be pivotal for phytoplankton bloom control (Townsend et al., 1994). In shallow coastal environments, vertical mixing may even raise phytoplankton mortality because of grazing by benthic filter-feeders (Cloern, 1996; Prins et al., 1996). In contrast, freshwater inputs from rivers may lead to a haline stratification in

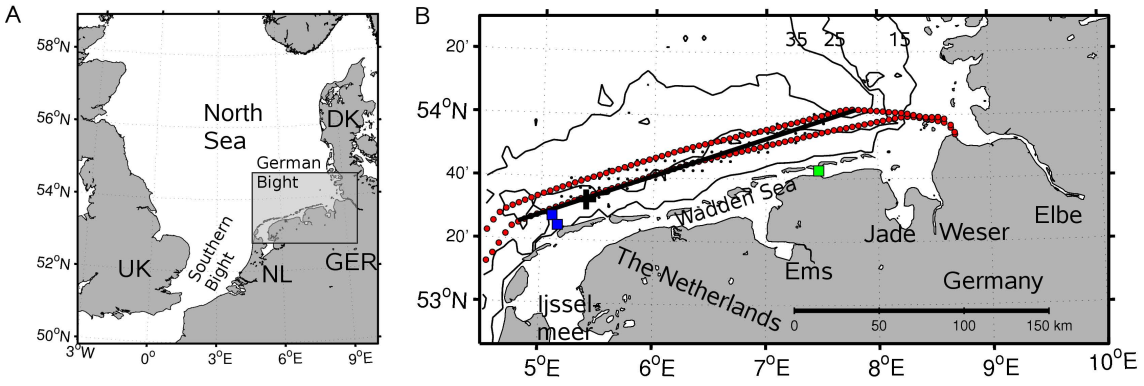

Fig. 1. (A) North Sea region including the study area (shaded). **(B)** Study area with the FerryBox route (red dots), the model transect (black line) and the release positions of the particles (black cross) at 5.4° E. Black dots indicate General Estuarine Transport Model (GETM) grid points used in the current analysis (see Fig. 3). Also shown are the coastal measurement pile (green square), nutrient measurement stations (blue squares) and depth contours (15, 25 and 35 m).

the vicinity of estuaries despite strong tidal currents or winds (Ragueneau et al., 1996).

Advection permanently changes the position and spatial structure of coastal water masses and links temporal variability to spatial gradients. It translates local growth or loss to commonly observed patchiness in phytoplankton distributions (Martin, 2003). Lucas et al. (1999b, 2009) have shown how lateral transport from a productive area can result in chlorophyll *a* (CHL-*a*) accumulation in an adjacent deep and unproductive channel proposing that spatial structures are either of local origin or a consequence of variable transport. Apart from the studies of Lucas et al. (1999a,b) in a shallow estuary, little is known about the interaction of advection with spatio-temporal variability in phytoplankton growth at intermediate to larger scales.

The range of potential factors affecting the development of a spring bloom considerably complicates the understanding of the phenomenon and its prediction as a response to physical forcing and biological interaction. In practice, already the detection of patterns in the CHL-*a* distribution or in other relevant variables is often limited by the availability and the resolution of data (Levin, 1992). Stationary time-series (e.g. Wiltshire et al., 2008) or singular ship-borne measurements are not sufficient to fully capture the temporal and spatial dynamics of processes in coastal seas. In the last two decades, however, satellite imagery added a wealth of data on surface water properties. It greatly facilitated the assessment of CHL-*a* variability (Thomas et al., 2003) and large-scale productivity estimates (Behrenfeld et al., 2005; Behrenfeld and Falkowski, 1997) and even proved useful to better understand trophic links in pelagic ecosystems (Platt et al., 2003). In temperate coastal seas and especially in the North Sea, however, high cloudiness strongly restricts the availability of data and often prevents the use of satellite imagery to detect fast biological dynamics on a scale of only a few days. High-frequency and time-continuous measurements by autonomous systems installed on ferries are filling this gap since recently. These FerryBoxes enable physical, chemical and biological observations along the one-dimensional tracks of a growing number of ships of opportunity, mostly sailing in European waters (Ainsworth, 2008). Here, we use data from a FerryBox that reveal significant differences in timing, location, and magnitude of the spring development along the continental coast of the German Bight, North Sea in 2004 and 2005 (Petersen et al., 2008).

Simulating phytoplankton dynamics, both in time and space, still challenges state-of-the-art ecosystem models. In the North Sea, Eulerian ecosystem models, which describe the evolution of their compartments on a fixed model grid, are able to reproduce typical cross-shore gradients in CHL-*a* in the Southern Bight (Lacroix et al., 2007) or the German Bight (Tian et al., 2009), but fail to simulate prominent characteristics inherent to the FerryBox data. Despite high-frequency hydrodynamic forcing and narrow grid spacing, these models are not able to generate significant alongshore variability, patchiness, and sharp temporal gradients. Besides imperfect model formulations, inadequate resolution of physical forcing (other than hydrodynamics) and numerical diffusion, which is unavoidable in Eulerian models, are potential explanations for the tendency of such models to underestimate the variability of biological state variables in coastal seas.

In this study, we take advantage of the high resolution of the FerryBox parameters sea surface temperature, turbidity and CHL-*a* and the ability of Lagrangian models to preserve steep gradients to simulate the observed evolution of CHL-*a* on an alongshore transect. A combination of the Lagrangian particle tracking method with an ecosystem model, which was introduced by Woods et al. (2005) for theoretical and educational purposes, allows an intuitive description of pelagic ecosystems consisting of many similar ensemble members that are advected by currents. With this approach, we simulate the development of the phytoplankton spring

blooms in 2004 and 2005. The main focus of this study lies on identifying the major factors that (1) triggered the onset of the spring bloom and (2) subsequently led to the distinct interannual differences between the CHL-*a* distributions of both years.

2 Study area

The study area is a section in the German Bight, off the German and Dutch North Sea coast, ranging from the Ijsselmeer in the west to the Elbe estuary in the east. It is limited by the intertidal Wadden Sea in the south and German Bight offshore waters in the north. For the purpose of this study, the area west of 6.5° E is refered to as the western part of the study area. Consequently, the area east of 6.5° E is the eastern part. Prevailing westerly winds (Siegismund and Schrum, 2001) and the counter-clockwise tidal wave result in an eastward mean current that closely follows the coastline (Staneva et al., 2009). Winds and tides also keep this shallow coastal sea with water depths below 40 m well mixed throughout most of the year. Several rivers (Fig. 1: Elbe, Weser, Ems, and Rhine through the Ijsselmeer) discharge into the German Bight supplying it with high nutrient loads (Beddig et al., 1997; Radach, 1992). Especially in the estuaries in the east, waters are highly turbid due to riverine suspended particulate matter. Waves and currents additionally enhance the resuspension of sediment from the soft bottom (Staneva et al., 2009) causing a steep turbidity gradient from the shore to the open sea and a high temporal variability of turbidity. Water temperatures range from close to zero in winter to values exceeding 20 °C during calm periods in warm summers (Wiltshire and Manly, 2004).
Phytoplankton in this region exhibits an articulate annual cycle with low winter production due to light limitation and low temperatures followed by a distinct spring bloom that is later terminated by nutrient limitation and grazing (Iriarte and Purdie, 2004). Often, a second phytoplankton bloom develops in late summer before light conditions prevent significant primary production. Thereafter, nutrients recover to maximum winter values (Loebl et al., 2009; Wiltshire et al., 2008).

3 Methods

3.1 Measured data

Most data presented in this study were measured by a FerryBox (Petersen et al., 2008, 2003) that was installed on a ferry sailing from Cuxhaven, Germany to Harwich, UK several times a week (Fig. 1). Availability and quality of the FerryBox variables temperature, turbidity and CHL-*a* restrict this study to the years 2004 and 2005. Prior to analysis, sea water is pumped from an inlet which is located approximately 5 m beyond the surface to the location of the system inside the ship hull. Turbidity and CHL-*a* are determined photometrically and fluorometrically, respectively. Depending on the species or the physiological state of phytoplankton, FerryBox CHL-*a* measurements may differ considerably from parallel analyses by high performance liquid chromatography see (see Petersen et al., 2008, for details). We nevertheless use this data because it is unmatched in resolution and because the range of CHL-*a* spanning more than two orders of magnitude is much greater than the potential error. Consequently, the focus regarding CHL-*a* is rather on distinct relative differences than on exact absolute values. Irradiance data was obtained from a measurement pile in the Wadden Sea, which is located on the eastern edge of the study area (Fig. 1, www.coastlab.org). Nutrient data from the FerryBox are not considered because of the unsatisfactory data coverage in the study period and their uncertain quality. Instead, phosphate data from two stations in the western German Bight (5.10° E, 53.46° N and 5.15° E, 53.41° E) are used. See Appendix for more details.
Zooplankton data from two sources (Continuous Plankton Recorder, D. Johns unpublished data, Renz et al., 2008) in the southern German Bight are used for a comparison with model results. For major mesozooplankton taxa (e.g. *Calanus*, *Temora*, *Centropages* or *Acartia*), individual counts are converted to concentrations in $\mu mol\,P \times l^{-1}$ based on published values for carbon content per individual and P:C ratios (Nielsen, 1991; Halsband-Lenk et al., 2001; Gismervik, 1997).

3.2 Model architecture

An individual-based model describes the physical and ecological dynamics of the phytoplankton in the study area. While transport due to advective processes is simulated by a Lagrangian particle tracking model, the dynamics of nutrients N, phytoplankton P and zooplankton Z is accounted for by an ecosystem model, which runs in each particle.
Hydrodynamics in the German Bight are driven by prevailing westerly winds and semi-diurnal tides resulting in a dominant alongshore, i.e. north-easterly or south-westerly, current. This feature is relatively stable throughout the year and becomes also evident in the analysis of currents generated by the General Estuarine Transport Model (GETM, Staneva et al., 2009; Stips et al., 2004), which is especially suited to simulate the hydrodynamics in tidally-dominated shallow seas. Significant correlations between the horizontal current components motivated a projection of the two-dimensional flow field onto the mean axis of transport (Fig. 3). In doing so, the model domain is reduced to a one-dimensional transect, while the general hydrodynamic properties are preserved. Furthermore, vertical homogeneity is assumed, since the study area is shallow with depths between 25 and 35 m and the water column is well-mixed during the period of interest in spring. This is supported by Joint and Pomroy (1993), who did not find vertical chlorophyll gradients within

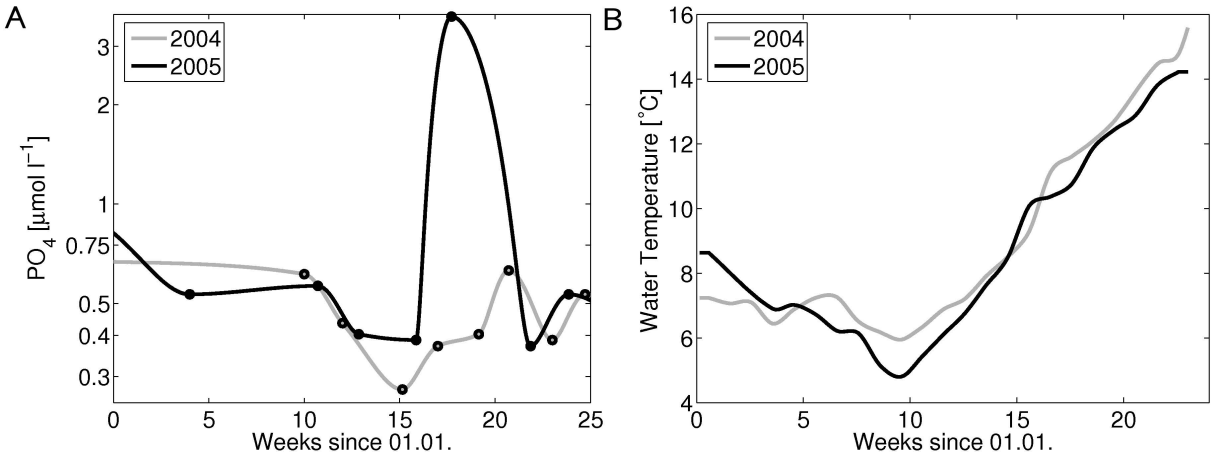

Fig. 2. (A) Phosphate in filtered surface water as the mean of measurements in the western German Bight (5.10° E, 53.46° N and 5.15° E, 53.41° E, fig. 1) in 2004 (grey line) and 2005 (black line) (source: DONAR database operated by the Dutch Ministry of Transport, Public Works and Water Management). **(B)** Weekly mean sea surface temperature, averaged between 5 and 8° E measured by the FerryBox in 2004 (grey line) and 2005 (black line).

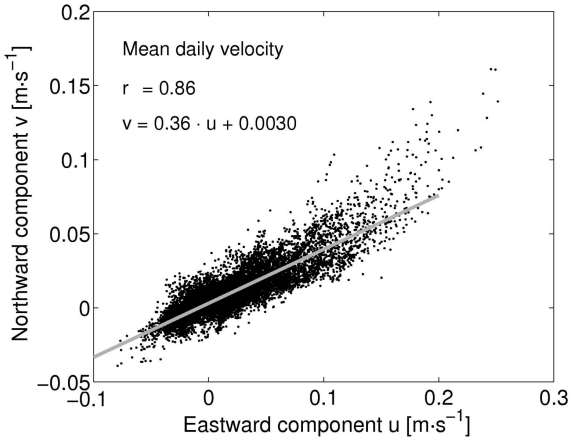

Fig. 3. Mean daily current components near the ferry route calculated by General Estuarine Transport Model (GETM) for the first 20 weeks in 2004. Considered GETM grid points are indicated as black dots in Fig. 1.

the euphotic zone at most sites in the North Sea.

Particles are transported by a particle tracking model, which uses the zonal component u of the mean daily current velocity generated by GETM while the meridional component v is defined as a linear function of u (see Appendix). A Lagrangian particle, thus, moves along the one-dimensional transect shown in Fig. 1. The entire simulation then consists of an ensemble of particles with different initial conditions (for N, P and Z) and particle trajectories, which are subject to different physical forcings (temperature, turbidity and photosynthetically active radiation PAR).

3.3 Ecosystem Model

Each particle carries a conceptualised ecosystem consisting of three compartments for one nutrient N, phytoplankton P and zooplankton Z. All variables are in phosphorus units. Primary production P_P is regulated by light following the approach of Ebenhöh et al. (1997). Furthermore, temperature and the availability of nutrients affect the production of phytoplankton biomass.

$$P_\mathrm{P} = \mu_P \cdot TPT \cdot NPT \cdot LPT \cdot P \tag{1}$$

where μ_P denotes the maximum growth rate of phytoplankton and *TPT*, *NPT*, and *LPT* are the production terms of temperature, nutrients and light, respectively. P_P links the consumption of nutrients to the growth of phytoplankton, which is additionally subject to zooplankton grazing P_Z. Thus, the model system describing the dynamics of all three compartments is given by

$$\frac{\partial N}{\partial t} = -P_\mathrm{P} \tag{2}$$

$$\frac{\partial P}{\partial t} = P_\mathrm{P} - P_Z \tag{3}$$

$$\frac{\partial Z}{\partial t} = \beta \cdot P_Z \tag{4}$$

with the zooplankton assimilation efficiency β. Since reported values (e.g. Edwards and Brindley, 1996; Conover, 1966) for β differ considerably between below 0.2 and higher than 0.9, a moderate value of 0.5 is chosen arbitrarily here. A more detailed model description is given in the Appendix. Because of the omission of detritus and, consequently, the remineralisation, the model systematically underestimates nutrient concentrations. To our understanding, this simplification is not critical, since nutrient concentrations remain above limiting levels during most of winter and spring.

4 Parametrisation, initial conditions and forcing

Every six hours a particle is released at 5.4° E during the first 20 weeks in 2004 and 23 weeks in 2005. Initial values for nutrient and phytoplankton concentrations are derived from measurements (Fig. 2). Phytoplankton biomass is converted from CHL-*a* data by means of two constant ratios. A Redfield C:P ratio and a Chl:C ratio of $0.3\mathrm{gCHL\text{-}}a \times (\mathrm{molC})^{-1}$ are assumed. The latter is in agreement with several measurements in the southern North Sea (Llewellyn et al., 2005; Geider, 1987). These authors, however, also clearly report a high variability in Chl:C and its dependence on several factors of which temperature, nutrient and light availability have been regarded as most important (Taylor et al., 1997; Cloern, 1995). Similar effects are known for C:P (Elser et al., 2000; Klausmeier et al., 2004). Fixing the the Chl:P ratio, thus, implies a strong simplification, which introduces a significant uncertainty into the model.

Zooplankton data are unavailable in the required spatial and temporal resolution at the position of initialisation. Instead, initial zooplankton biomass at the initial position x_0 is estimated as a fraction of the phytoplankton biomass at a previous time (see Eq. A11). During the first half of the year, the assumption of zooplankton lagging behind phytoplankton is a well documented feature in marine ecosystems, which was also reported from the nearby time-series station of Helgoland roads (Greve et al., 2004). Later in the year, however, the zooplankton initialisation clearly loses its validity. After initialisation, the evolution of the three ecosystem variables is determined by the water depth ζ, the water temperature T, and the light climate. T and ζ are derived from FerryBox measurements and the GETM bathymetry, respectively. The light climate is calculated using hourly surface PAR I_0, which is derived from incident irradiance data from a measurement pile, and measured turbidity (Fig. 5, cf. Appendix). Most parameter values have been manually calibrated within known ranges and according to literature values (Table 1). Four sensitive parameters (I_{opt}, k_N, k_P and Z_{min}) that were identified manually, however, are calibrated with the objective of (1) maximising the lateral CHL-*a* gradient along the transect in 2005, and (2) minimising the gradient in 2004 (cf. Fig. 4). The model is, hence, calibrated to reproduce the two qualitatively different CHL-*a* regimes in 2004 and 2005 with identical parameter sets. Therefore, the simulated ratio of mean CHL-*a* in two neighbouring regions during the spring bloom is calculated and compared to the ratio derived from measurements.

5 Results

5.1 Measured spring bloom dynamics

A continuous spring bloom was detected by the FerryBox throughout the study area in 2004 (Fig. 5). Starting in the western part in week 12, a patch with CHL-*a* concentrations above $30\,\mu\mathrm{g\,l^{-1}}$ developed eastward within six weeks. Measured turbidity data exhibit an inverse pattern (Fig. 5). While winter values fluctuated considerably between 2 and 10FTU, the variability decreased throughout spring and values below 3FTU indicate good light availability. The spatial and temporal extend of the minimum in turbidity closely resembles the pattern of maximum CHL-*a* . Low temperatures did not prevent the growth of phytoplankton, as the onset of the spring bloom around week 12 in 2004 coincided with the coldest period in this year (Fig. 2). Thereafter, temperature was steadily rising as was CHL-*a* .

Though phosphate data are relatively sparse compared to Ferrybox measurements, it nonetheless outline the high temporal dynamics of phosphate during spring (Fig. 2). After a steep decrease from winter values phosphate concentrations already marked a turning point around week 15, which was followed by a significant recovery until week 20.

In 2005, an articulate bloom with CHL-*a* above $20\,\mu\mathrm{g\,l^{-1}}$ only occurred in the western part of the study area (Fig. 5). Measured CHL-*a* rarely exceeded $5\,\mu\mathrm{g\,l^{-1}}$ further east between 6.4° E and 7.5° E. Unlike in 2004, patterns of high CHL-*a* concentrations were associated with high turbidity in 2005 and the minimum of turbidity already occurred before the onset of the spring bloom between week 12 and 15. After phosphate concentrations decreased slightly during the initial phase of the bloom, exceptionally high values exceeding $3\,\mu\mathrm{mol\,l^{-1}}$ were measured during the maximum of the bloom in week 18 (Fig. 2).

5.2 Model calibration

A systematic variation of the four parameters I_{opt}, k_N, k_P and Z_{min} reveals considerable robustness of the obtained CHL-*a* patterns with respect to uncertain parameters. While absolute values of CHL-*a* are strongly depending on the parametrisation, the ratio of CHL-*a* concentrations in two zonally adjacent areas turned out to be rather consistent (see Fig. 5 for the definition of the areas) indicating that a different mechanism was dominant in each of the years. The location of the areas was determined manually to properly capture the spring bloom characteristics in time and space.

In 2004, there is only a weak spatial gradient in the measured data and the simulations reveal a mean ratio close to 0.7, i.e. slightly higher CHL-*a* values in the west than in the east (Fig. 4). In the following year, the measured ratio indicates distinctively higher CHL-*a* concentrations in the west than in the east and the simulations resemble that relation with a mean value below 0.4. The ratio is very insensitive

Table 1. Model parameters and their values (see also Appendix).

Symbol	Definition	Value	Unit	Ref.
a	Light extinction parameter	0.15	$[m^{-1} \times FTU^{-1}]$	Devlin et al. (2008)
b	Extinction offset	0.05	$[m^{-1}]$	Devlin et al. (2008)
β	Zooplankton assimilation efficiency	0.5	[ ]	Edwards and Brindley (1996); Conover (1966)
I_{opt}	Scaling parameter of the *p/I*-curve	225	$[W \times m^{-2}]$	Model calibration
C:P	Carbon to phosphorus ratio	106	$[molC \times (molP)^{-1}]$	Redfield ratio
Chl:C	CHL-*a* to carbon ratio	0.3	$[gCHL\text{-}a \times (molC)^{-1}]$	Faure et al. (2006) Llewellyn et al. (2005) Geider (1987)
k_N	Half-saturation of nutrients limitation	0.5	$[\mu molP \times l^{-1}]$	Model calibration
k_P	Half-saturation of grazing	0.75	$[\mu molP \times l^{-1}]$	Model calibration
μ_p	Phytoplankton maximum growth rate	0.69	$[d^{-1}]$	Cloern (1995); Furnas (1990)
μ_z	Zooplankton maximum growth rate	0.56	$[d^{-1}]$	Stelfox-Widdicombe et al. (2004)
$Q_{10,P}$	Temperature sensitivity zooplankton	3.0	[ ]	Raven and Geider (1988)
$Q_{10,Z}$	Temperature sensitivity phytoplankton	2.0	[ ]	Hansen et al. (1997)
r_{PAR}	Ratio between incident irradiance and PAR	0.5	[ ]	Ebenhöh et al. (1997)
r_Z	Initial zooplankton fraction	0.04	[ ]	
τ_Z	Time lag for zooplankton initialisation	14	[d]	
T_0	Reference temperature	10	[°C]	
Z_{min}	Minimum zooplankton biomass	0.0075	$[\mu molP \times l^{-1}]$	Model calibration

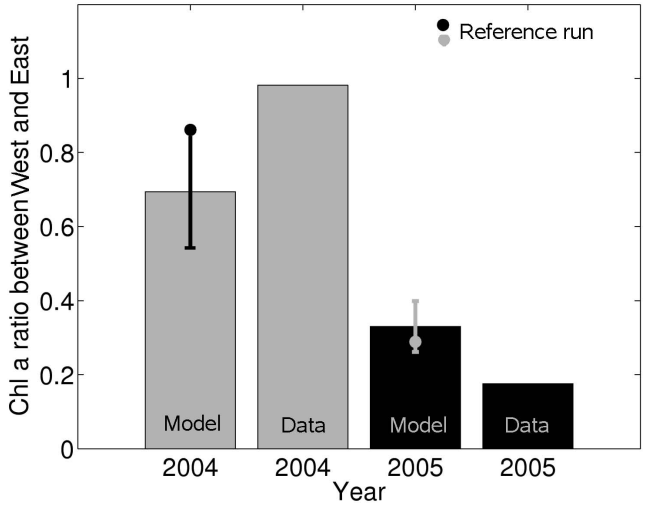

Fig. 4. Sensitivity of model results to the systematic variation of four parameters ($I_{opt}[125...225 W \times m^{-2}]$, $k_N[0.3...0.7 \mu molP \times l^{-1}]$, $k_P[0.25...0.9 \mu molP \times l^{-1}]$ and $Z_{min}[0.0075...0.015 \mu molP \times l^{-1}]$) regarding the zonal gradient in CHL-*a* . The gradient is expressed as the ratio of mean CHL-*a* concentrations in two adjacent areas as shown in Fig. 5. Values below one indicate higher CHL-*a* in the west than in the east. Error bars show the standard deviation of a total of 162 model runs, solid circles denote the ratios of the reference run. Data bars display the same ratio derived from FerryBox measurements.

to variations of the four variable parameters included in the model calibration. The selected reference parametrisation given in Table 1 is not optimal for reproducing the CHL-*a* data in each of the years, but presents a compromise to simulate qualitatively different phytoplankton dynamics in two consecutive years with a constant set of parameters. Following model results have been produced with this reference parameter set.

5.3 Bloom control by light climate in 2004

The model produces an articulate spring bloom extending over the entire longitudinal range of the study area in 2004 (Fig. 5). In the west, where the phytoplankton bloom develops earliest around week 11, CHL-*a* already declines again at the end of the simulation, while phytoplankton is still growing in the eastern part of the German Bight. While the timing of the spring bloom is closely matched, maximum concentrations of around 30 $\mu g\, l^{-1}$ east of 6.4° E are slightly underestimated by the model. As in the data, the phase of strong phytoplankton growth initiates shortly after a sharp drop in turbidity from above 3FTU to 1.5FTU (Fig. 6). In contrast, the drop in the light production term (LPT) at the end of the bloom period is, however, not linked to turbidity but to low incident irradiance.

Primary production in the model is mostly determined by the availability of light and nutrients. While the distribution of the LPT closely resembles the chlorophyll distribution, the nutrient production term (NPT) indicates only negligible nutrient limitation until week 16 (Fig. 5). Later, the NPT reaches growth-limiting values close to zero only west

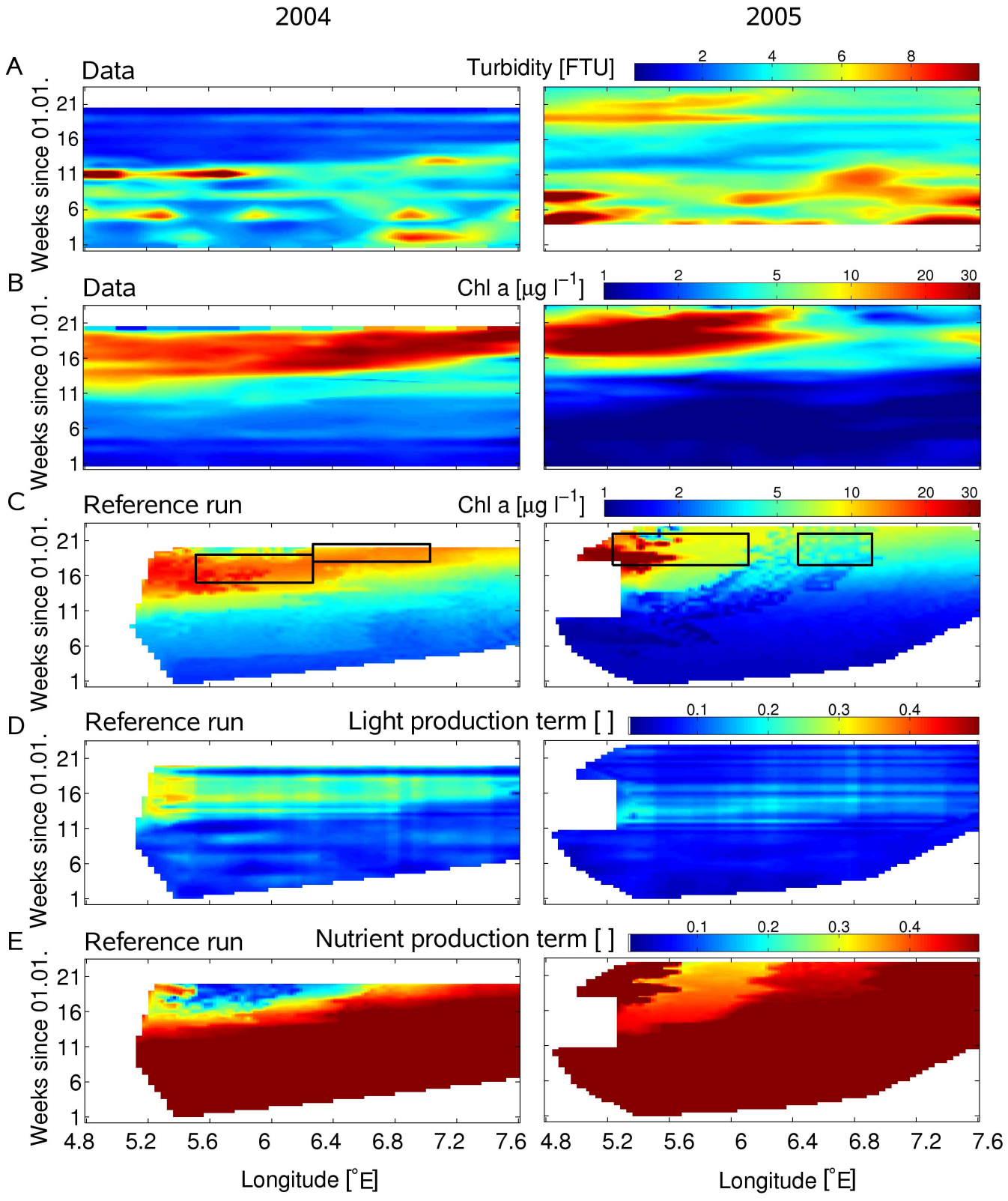

Fig. 5. **(A)** Turbidity measured by the FerryBox between Cuxhaven, Germany and Harwich, UK in 2004 and 2005 (Fig. 1); See Appendix for more details on the data treatment. **(B)** CHL-*a* measured by the FerryBox (cf. A). **(C)** Simulated CHL-*a* concentration; squares indicate areas that are used to calculate the CHL-*a* gradient for the sensitivity study (see Sect. 3 for more details); the data gap at the western edge in 2005 is due to missing particle coverage. **(D)** Simulated light production term (Eq. 1, A5). **(E)** Simulated nutrient production term (Eq. 1, A5).

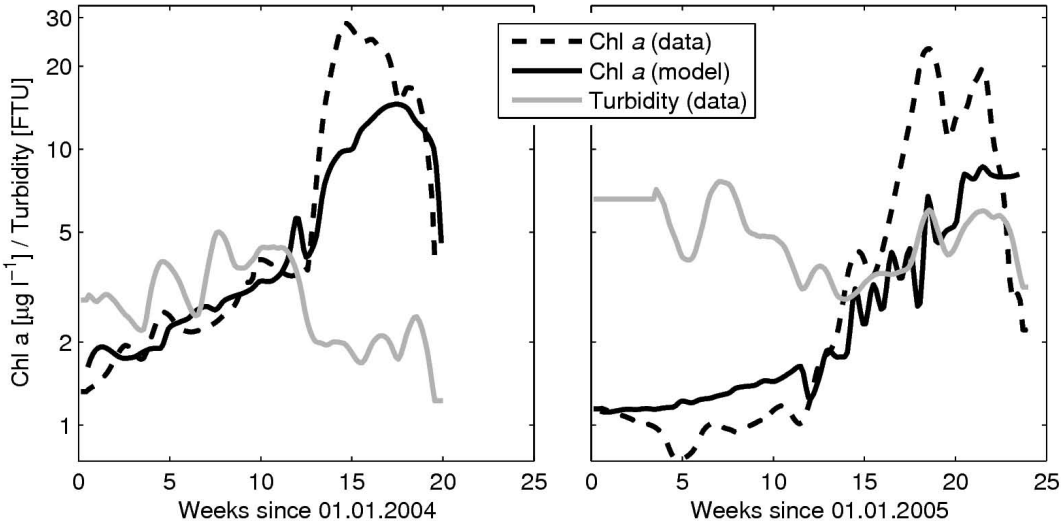

Fig. 6. Measured (black dashed) and simulated (black solid) CHL-*a* and measured turbidity (grey) at 6.2° E.

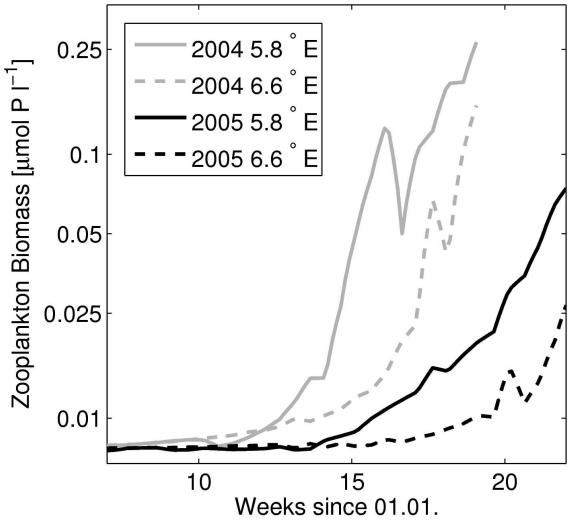

Fig. 7. Simulated zooplankton biomass in µmol P × l^{-1} at two locations in 2004 (grey) and 2005 (black).

of 6.4° E. Zooplankton (Fig. 7) has a minor impact on the onset of the phytoplankton bloom. However, strong grazing causes the collapse of the phytoplankton bloom after the exhaustion of nutrients in the western part. Similar to phytoplankton, zooplankton growth begins earlier in the west.

5.4 Bloom advection in 2005

No spatially continuous plankton bloom develops during the first 23 weeks of 2005. Simulated CHL-*a* exceeds 30 µg l^{-1} only in the vicinity of the initial particle position at 5.4° E in late spring. Nonetheless, the patch of elevated CHL-*a* values, extending from the western border of the study area to approximately 6.4° E, is also reproduced by the model, albeit less pronounced than in the measurements. While the model clearly underestimates enhanced growth rates between week 15 and 18, the temporal dynamics of phytoplankton including the timing of the spring bloom is well captured (Fig. 6). In the last weeks of simulation, phytoplankton biomass is still growing when measurements already indicate the collapse of the bloom (week 22–23).

Although light conditions begin to improve between week 12 and 16, they never reach the favourable levels observed in 2004 (Fig. 5). Indeed, the LPT even falls back to low winter values close to 0 in the west. In this year, high turbidity exceeding 4FTU is significantly impairing light availability so that the increase of incident irradiance is not noticeable in the LPT. In contrast to light conditions, nutrient availability does not limit the growth of phytoplankton in 2005. Similar to 2004, zooplankton biomass is highest in the western part of the study area, i.e. occurring together with high phytoplankton biomass. Absolute values do not exceed 0.05 µmol P× l^{-1} until week 20.

By resolving the path of single trajectories it is possible to assess the role of hydrodynamics in the development of spatial patterns in the CHL-*a* distribution (Fig. 8). All particles that are located east of 6.3° E after week 15 have been initialised with rather low CHL-*a* values during the first weeks of 2005 and stayed in the coastal waters off the Wadden Sea coast during the entire simulation period. Algal biomass of the majority of these particles does never exceed 7 µg CHL-*a* l^{-1} because low light availability prevents higher productivity (Fig. 5). In contrast, water masses that form the high CHL-*a* patch west of 6.3° E entered the study area during a period of strong eastward drift within only a few days (small circle in Fig. 8). Along with this eastward inflow in week 14, the measured CHL-*a* at the

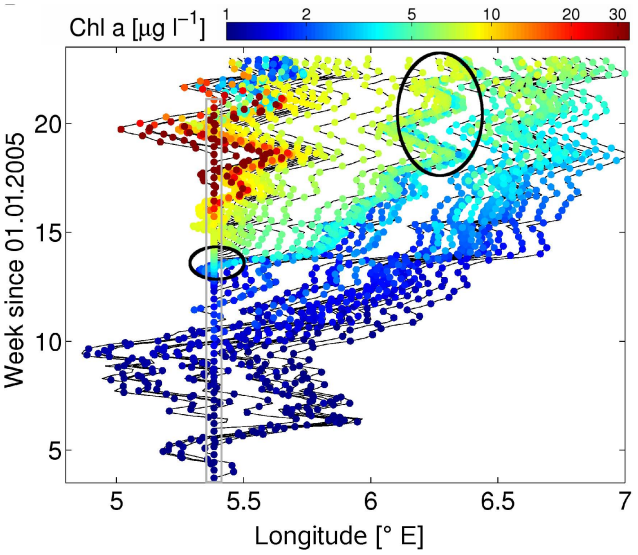

Fig. 8. Model trajectories coloured according to their simulated CHL-*a* values; all particles are released at 5.4° E. The small ellipse marks the eastward inflow of a water mass with elevated phytoplankton concentrations; the big grey circle indicates the fate of the first particles released within the small circle that later in the spring bloom form the border between a high and a low CHL-*a* region.

initial position rises severalfold. The trajectories originating during this event later constitute the eastern envelope of the high CHL-*a* patch. Furthermore, they even resemble the characteristic two-tailed shape of the CHL-*a* maximum between 6.0 and 6.5° E (big grey circle in Fig. 8), which is also evident in the data between week 18 and 21 (Fig. 5).

To summarise, growth conditions in the study area are rather homogeneous throughout the study area in 2005. The division between high CHL-*a* in the west and significantly lower concentrations in the east can therefore be attributed to a pronounced eastward drift importing high CHL-*a* waters from the adjacent Southern Bight into the western German Bight. To further substantiate the influence of hydrodynamics on the mesoscale bloom structure, the simulation for 2005 is also conducted with the 2004 currents (Fig. 9). All other forcing and boundary conditions remain unchanged in this set-up. The results of this model set-up clearly fail to generate the steep CHL-*a* gradients observed in the data. Hydrodynamics in 2004 lack the pronounced inflow that causes the eastward advection of particles with high initial CHL-*a* values far into the central areas of the study area.

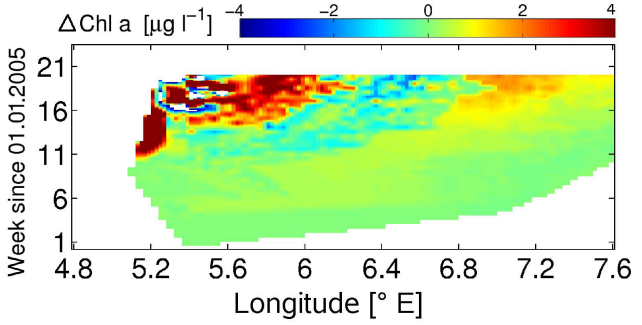

Fig. 9. Differences in CHL-*a* between the reference run in 2005 and the same run with 2004 hydrodynamics. Deviations are only attributable to differences in the current system.

6 Discussion

Despite the model's simplicity regarding spatial resolution and ecosystem structure, it is capable of reproducing the general spatio-temporal distribution of CHL-*a* in the coastal German Bight as measured by the FerryBox on the Cuxhaven - Harwich ferry in 2004 and 2005. More important, our results suggest that different mechanisms - turbidity dynamics and variability of alongshore currents – triggered the onset of the spring bloom and led to the observed mesoscale differences in blooming patterns of phytoplankton in the two years.

6.1 Light climate

Typical for phytoplankton in temperate coastal seas, the 2004 spring bloom was triggered by a change in the light climate (Weston et al., 2008; Iriarte and Purdie, 2004; Cloern, 1996). Besides increasing solar irradiance, especially a drop in turbidity greatly improved growth conditions for autotrophs in April of this year. While surface incident PAR approached $2000 \mathrm{Wh} \times \mathrm{m}^{-2} \mathrm{d}^{-1}$ in April, the mean water column PAR exceeded $200 \mathrm{Wh} \times \mathrm{m}^{-2} \mathrm{d}^{-1}$ after the sharp drop in turbidity in week 12. Later, the mean water column PAR also reached $400 \mathrm{Wh} \times \mathrm{m}^{-2} \mathrm{d}^{-1}$ on days with high incident irradiance corroborating Iriarte and Purdie (2004) who observed strong phytoplankton growth above this level of mean water column PAR. Turbidity in coastal seas can, in general, be related to winds, tides, and suspended particulate matter input from rivers (Iriarte and Purdie, 2004; May et al., 2003; Cloern, 1996), but it may also be raised by planktonic organisms in the water column (Tilzer, 1983). It is beyond the scope of this study to explicitly assess the role of different factors in leading to the rapid decrease of turbidity. However, weak winds from easterly directions in weeks 15 to 19 likely favoured the clearance of the water column (data from Wadden Sea measurement pile, not shown). The consequences of ceasing light limitation are accurately predicted by the model, in particular with respect to the spring bloom timing throughout the entire study area. The rapid response of phytoplankton to changes in the available light resource,

both in the data as well as in the model, thus, corroborates the pivotal role of suspended particulate matter in controlling coastal spring blooms, at least in some years (Tian et al., 2009).

In contrast to 2004, there is no clear negative correlation between CHL-*a* and turbidity in the data in 2005. Instead maximum CHL-*a* levels have been observed in highly turbid waters. Despite comparable surface incident PAR values to 2004, mean water PAR remained significantly below $200\mathrm{Wh} \times \mathrm{m}^{-2}\mathrm{d}^{-1}$ inhibiting phytoplankton growth in May 2005. The turbidity distribution, hence, fails to explain the observed CHL-*a* pattern in this year. We therefore conclude that the local light climate is the key factor for the spring bloom development in 2004. Local light conditions are, however, not sufficient to understand and predict the dynamics of the spring bloom in all years.

6.2 Hydrodynamics

The spatial and temporal distribution of CHL-*a* in 2005 was significantly affected by advection underlining the importance of the circulation for modelling ecosystems in highly dynamic coastal seas (Skogen and Moll, 2005). In this year, the analysis of simulated particle trajectories clearly reveals the eastward inflow of a distinct water mass with an elevated CHL-*a* concentration. With different hydrodynamics the model fails to reproduce the observed development of the fundamentally different CHL-*a* regimes in 2005. The inflow hypothesis is further backed by FerryBox salinity data (not shown), which indicate the eastward intrusion of a more saline water mass into the western part of the study area in May. Furthermore, Petersen et al. (2008) presented a series of MERIS satellite derived CHL-*a* maps of the southern North Sea showing the growth and transport of a chlorophyll patch from the Rhine estuary to the western German Bight.

Our results demonstrate that ecosystem dynamics in the coastal German Bight can be distinctively influenced by processes in the adjacent Southern Bight under specific hydrodynamic conditions. Hydrodynamic events can bring together water masses with very different history and biochemical signature and, as a consequence, lead to the development of steep gradients. FerryBox data as well as our model results also indicate that such gradients may persist in the coastal German Bight despite high current variability.

6.3 Nutrients

Despite the reduction of riverine nutrient inputs into the southern North Sea in the last decades, high winter values still provide favourable conditions for primary producers in the German Bight (Cadée and Hegeman, 2002). The results from 2004 underline the crucial role of initial, i.e. winter, nutrient concentrations for the spring bloom since the simulated phytoplankton biomass is built up using solely the initial amount of phosphate in the Lagrangian particles. The crucial role of phosphate in the Southern and the western German Bight motivates the usage of phosphorus as the currency of the ecosystem model (Loebl et al., 2009). Silicate availability may also become a driving factor as diatoms typically prevail before mass occurrence of *Phaeocystis* (see below and Peperzak et al., 1998). It is noteworthy, however, that the results do not critically depend on the choice of the macronutrient, since the model only accounts for one very generic phytoplankton organism.

Though the remineralisation of nutrients through the microbial loop and the benthic-pelagic coupling as well as additional nutrient inputs from rivers are all neglected, the model is nevertheless able to reproduce the general spring bloom pattern of phytoplankton in both years. We, hence, conclude that these processes only have a minor importance for algal growth during spring and that their effect can be compensated by setting a reference Chl:P ratio which is potentially overestimating values during spring. While nutrients are not affecting the timing or the spatial distribution of the spring bloom, their limitation clearly determines its duration in the coastal German Bight in most of the years (Loebl et al., 2009; Kuipers and van Noort, 2008; van der Zee and Chou, 2005; Skogen et al., 2004). Also the amplitude of the bloom is depending on incipient nutrient concentrations. The tendency of the model to underestimate measured CHL-*a* levels can therefore be attributed to the omission of remineralisation processes or additional riverine nutrient inputs, at least in 2004. In contrast, it is not nutrient supply but light availability that limits simulated phytoplankton growth in 2005.

6.4 Grazing

In the simulation, strong grazing on phytoplankton occurs towards the end of the spring bloom finally causing the collapse of phytoplankton biomass. In contrast, zooplankton had no significant impact on the timing of the spring bloom. This finding is also supported by Loebl and Beusekom (2008) who describe a strong seasonality of microzooplankton in the coastal German Bight with low grazing pressure in early spring. Along the spatial domain, zooplankton concentrations are higher in the west than in the east in both years, closely resembling the pattern of phytoplankton. There is, however, no evidence that the spatial heterogeneity of grazing caused the observed gradients in CHL-*a* . Rather, zooplankton minimises phytoplankton gradients in the model.

Given the scarcity of measurements, the validation of the simulated zooplankton dynamics remains fragmentary. In April and May 2004, estimated data of major mesozooplankton species from the Continuous Plankton Recorder Survey (CPR) provided by D. Johns reveal values below $0.05\,\mu\mathrm{mol\,P} \times\ \mathrm{l}^{-1}$ in the western German Bight (5.4° E). Moreover, the temporal and spatial pattern of secondary production of *Pseudocalanus elongatus*, a dominant zooplankton species in the coastal German Bight, along the FerryBox route in spring 2004 (Fig. 7, Renz et al., 2008) support the

findings of this study. Similar to the model results, measured data reveal a steep increase of secondary production in May and June and highest values in the western German Bight. The biomass of *P. elongatus* have been estimated to be less than 0.1 µmol P× l^{-1}.

Considering the large uncertainties associated with the conversion of individual counts to P concentrations, the simulated zooplankton dynamics are a fair representation of measured data during most of the simulation period. Only in the decay phase of the spring bloom the model significantly overestimates measured mesozooplankton concentrations, even when considering that the estimates do not include microzooplankton. The biomass of the latter is typically one order of magnitude lower than the biomass of mesozooplankton, but occasionally reaches similar values during the spring bloom (Sommer and Lengfellner, 2008). The simulated overestimation of zooplankton towards the end of the simulation period, which is caused by the lack of a loss term in the zooplankton growth equation (cf. Eq. 4), does, however, not influence either the timing or the spatial extent of the spring bloom.

The model does not explicitly consider either different numbers of overwintering zooplankton or meroplankton, which can be abundant in coastal waters during spring and summer (Smetacek and Cloern, 2008). While the temperature dependence of zooplankton growth (cf. Eq. 4) implicitly accounts for the positive effect of higher temperature on zooplankton overwintering success, there is no mechanism describing meroplankton dynamics. Variability in winter zooplankton concentrations leads to spatially uniform differences in grazing pressure in the model, which does only slightly affect the beginning of the bloom or spatial gradients of phytoplankton. In contrast, meroplankton, which can be related to less saline coastal waters, selectively increase grazing on phytoplankton in certain water bodies. The absence of a phytoplankton bloom in the eastern part of the study area in 2005 may, thus, be explainable with strong meroplankton grazing, which only occurred in the coastal water body, but not in the more saline waters in the western part of the FerryBox route. The simulation of highly variable meroplankton is, however, not compatible with the simple approach of this study requiring specific models that also include adult stages of benthic invertebrates (e.g. Brandt et al., 2008).

6.5 Algal community structure and stoichiometry

Despite the general agreement with observations, the model results lack few features inherent to the data. The simulated phytoplankton growth, for example, is slower during the first weeks of the spring bloom than the measurements suggest in 2004. This mismatch is partly due to specific model formulations. The multiplication of terms in the formulation of the primary production (Eq. 1) clearly leads to a conservative estimate compared to other approaches (e.g. the Liebig law of the minimum or temperature independence of the initial slope of the P/I-curve Geider et al., 1998).

Another origin of model errors can be associated to simplifications in the ecosystem model that neglects the intrinsic variability of all considered compartments (i.e. nutrients, algae and herbivores). Wirtz and Eckhardt (1996) have shown the critical relevance of variable traits in modelling multispecies phytoplankton communities. Intracellular element ratios are key variables of algal physiology that also affect all model–data comparisons. The reported ranges of variability of the two stoichiometric ratios Chl:C and C:P, for example, clearly exceed the deviations between simulated and measured CHL-*a* data in this study (Llewellyn et al., 2005; Hecky and Kilham, 1988; Geider, 1987; Tett et al., 1985). Much of the unexplained deviations between model and data could be therefore attributed to errors of the fixed intracellular element ratios. The motivation for using static element ratios notwithstanding is twofold. Firstly, it is still an ongoing effort to represent the underlying mechanisms causing these fluctuations in ecosystem models (Pahlow, 2005). Besides, there is no data available to constrain simulated element ratios in this study. Secondly, the main purpose of the model is to simulate the onset and development of the spring bloom. For this short period of the year when nutrients are replete and phytoplankton is light limited, the strong assumption of constant element ratios is reasonable. In addition, this simplistic assumption allows a better comparison of the impact of physical forcing on the phytoplankton dynamics in both years.

Another important and variable trait is the optimal irradiance I_{opt} (Macedo et al., 2001). Changing photosynthetic characteristics do not only matter when simulating the course of a bloom, but may also be relevant for understanding interannual differences. In 2005, the underestimation of CHL-*a* in the western part can be attributed to an overrated light limitation that is caused by the selection of a too large I_{opt}. It appears therefore possible that diatoms, which have lower light requirements, e.g. a lower I_{opt}, than *Phaeocystis*, dominated the spring bloom in this year (cf. Wiltshire et al., 2008). Observations in the Dutch Wadden Sea in 2004, however, identified *Phaeocystis* to be the dominating species during April (Kuipers and van Noort, 2008). Higher numbers of diatoms were only observed thereafter in May. It is likely that *Phaeocystis* was able to outcompete diatoms already early in 2004 because of the exceptionally high light availability after week 12.

Neglecting variable stoichiometry and different light requirements clearly limits the model's capabilities to exactly reproduce the measured data. This simplistic approach reveals, however, that most of the observed mesoscale CHL-*a* pattern can be reproduced by using high resolution physical boundary conditions and forcing. To address the still unexplained part of the observed dynamics in CHL-*a* , more complex ecosystem models, which better account for biological variability, are clearly more appropriate.

6.6 1-D Lagrangian modelling

The simplified approach of using moving particles along a one-dimensional projection entails several advantages: The transect matches the two adjacent ferry routes, making reliable physical forcing data and fluorescence measurements available. This is particularly important as results indicate that mesoscale variability originates from high-frequent fluctuations of ambient conditions. Of course, an extrapolation of simulated values to a larger area beyond the transect would require a different approach.
Advantages of the Lagrangian over the more common Eulerian approach also comprise the ability to preserve strong gradients and the possibility to easily assess the particle history, which greatly enhanced the understanding of the spring bloom development in 2005. Furthermore, the one-dimensional approach entails a greatly reduced computational effort compared to higher-dimensional set-ups, facilitating parameter calibration and sensitivity studies (Soetaert and Middelburg, 2008).

7 Conclusions

In this study, we identified two different mechanisms explaining the observed spring dynamics of phytoplankton in a coastal marine ecosystem. In 2004 the build-up of CHL-*a* is determined by a significant drop in turbidity. In contrast, detailed knowledge of the history of individual water masses is essential to understand the phytoplankton dynamics in 2005. Under severe light limitation due to high turbidity, the spring bloom was triggered by the import of water masses containing higher phytoplankton concentrations.
The successful simulation of fundamentally different spring bloom dynamics in two consecutive years with constant parameters demonstrates the appropriateness of this simple coupled model for analysing the origin of mesoscale CHL-*a* patterns in spring blooms. Against the common trend of building ever more complex models, the reduction of hydrodynamic information to a low-pass filtered horizontal transect facilitates the understanding of mesoscale structures along the shore. The availability of high-frequent FerryBox data has thereby proven to be paramount. In this context, the attempt to reproduce time-series data of dynamic coastal systems without taking into account horizontal transport appears to be at least difficult. A satisfying correlation between ecosystem dynamics and local conditions in one period does not guarantee its validity in other time intervals. It remains surprising, however, that the reproduction of alongshore variability is relatively successful despite the ignorance of cross-shore processes in this tidally-dominated coastal sea.
Though our coupled Lagrangian ecosystem model is able to simulate the basic dynamics of the plankton community, it is obviously limited to the winter and spring period. Many assumptions, e.g. the ignorance of remineralisation processes or adaptation in algal stoichiometry and/or community structure, have to be reconsidered prior to a potential application to the entire season.
Our study also underlines the relevance of time-continuous as well as spatially explicit data of herbivores including microzooplankton. A more extensive combination of operational FerryBox and CPR measurements would be, thus, an important step towards an effective characterisation of ecosystem dynamics in a regional shelf sea like the North Sea.

Appendix A

A1 Data integration

The considered FerryBox variables were measured by the following devices (analyser, manufacturer, country): Temperature T[°C] (PT100, FSI, USA), turbidity Tb[FTU] (CUS31W2A, Endress & Hauser, Germany), salinity S[PSU] (EXCELL, FSI, USA), and chlorophyll a (CHL-*a*) [$\mu g\,l^{-1}$] (SCUFA-II, Turner Design, USA). The original resolution of the data is approximately 100 m depending on the speed over ground of the vessel. When operating scheduled, the ferry passed the study area once a day, mostly in the evening or at night. All measured data are binned in time and space with a bin size of 7d and 0.2° to eliminate high frequency fluctuations and to fill smaller data gaps. By interpolating these coarse distributions to a higher resolution grid with a bin size of 1d and 0.02° smooth and consistent distributions are generated (Fig. 5). Data gaps are filled with the nearest available value in time, since a failure of a measurement device normally leads to missing data along the entire spatial domain.
Incident irradiance data are composed from pile data recorded at 7.47° E, 53.71° N in the Wadden Sea during spring and summer (source: www.coastlab.org) and synthetic values derived with the astronomic method described by Ebenhöh et al. (1997) for data gaps, which occur mainly in winter when the pile is not operating. Phosphate was measured in filtered surface water 4 and 10 km off the coast in the western German Bight (5.10° E, 53.46° N and 5.15° E, 53.41° E) approximately once a month (source: database DONAR operated by the Dutch Ministry of Transport, Public Works and Water Management, www.waterbase.nl).

A2 Model architecture

The linear regression of vertically integrated, mean daily currents produced by a 3 nm set-up of the General Estuarine Transport Model (GETM) reveals a significant correlation between their zonal and the meridional components (u and v) in the vicinity of the ferry route (2004: Pearson $r = 0.86\,p < 0.01$, 2005: $r = 0.81\,p < 0.01$, vertically integrated daily mean currents during the first 140 days of the

respective year, Fig. 1). Hence, daily mean currents are directed either to the north-east or to the south-west. The reliability of this projection, however, declines outside the range between 5.2° E and 7.5° E where the correlation is calculated. The particle tracking algorithm uses the mean daily zonal velocity component u generated by GETM to compute the meridional velocity component v

$$v = a \cdot u + b \tag{A1}$$

with the parameter values $a = 0.349$ and $b = 0.003\mathrm{m} \times \mathrm{s}^{-1}$ derived by linear regression (first 140d of both years). In the following, b is neglected for its smallness. The current velocity w along the model domain at position x and time t is hence solely a function of u and given by

$$w(t,x) = \sqrt{u^2(t,x) + v^2(t,x)} \tag{A2}$$

$$= \sqrt{1+a^2} \cdot u(t,x) \tag{A3}$$

resulting in the change of position of particle i

$$dx(t,x_i) = w(t,x_i) \cdot dt. \tag{A4}$$

An explicit fifth-order Runge-Kutta algorithm is applied to integrate Eq. (A4).

A3 Ecosystem model

P_P denotes the primary production of phytoplankton

$$P_P = \mu_P \cdot \overbrace{\epsilon_P}^{\text{Temperature}} \cdot \overbrace{\frac{N}{N+k_N}}^{\text{Nutrients}} \cdot \overbrace{\frac{1}{k_z \cdot \zeta} \cdot \int_{x_D}^{x_0} \frac{4}{1+4 \cdot x} dx}^{\text{Light}} \cdot P \tag{A5}$$

with the maximum growth rate μ_p, the half saturation constant for nutrient uptake k_N, the light attenuation coefficient k_z, and the water depth ζ. The labelled terms in Eq. (A5) are the dimensionless terms for the utrient production (NPT) and the light production (LPT) and the temperature production (TPT). Following Ebenhöh et al. (1997), the depth integral of the *p/I*-curve i dimensionless with

$$x_0 = \frac{I_0}{I_{\mathrm{opt}} \cdot \epsilon_P} \tag{A6}$$

$$x_D = \frac{I_D}{I_{\mathrm{opt}} \cdot \epsilon_P} \tag{A7}$$

where I_0 and I_D are the photosynthetically active radiation (PAR) at the surface and the bottom, respectively. PAR is assumed to be a constant fraction $r_{\mathrm{PAR}} = 0.5$ of the incident irradiance (Ebenhöh et al., 1997). The corresponding p/I-curve is a Monod function with the scaling parameter I_{opt}.

All biological processes dependent exponentially on the water temperature T

$$\epsilon_X = Q_{10,X}^{(T-T_0)/10} \tag{A8}$$

with $Q_{10,X}$ determining the sensitivity to changes in T and the temperature T_0 at which $\epsilon_X = 1$. The subscript X stands for either P (phytoplankton) or Z (zooplankton).
Observational evidence supports the use of a Holling-type III functional response to simulate the zooplankton grazing P_Z on phytoplankton (Gentleman et al., 2003; Verity, 1991).

$$P_Z = \epsilon_Z \cdot \mu_Z \cdot \frac{P^2}{P^2 + k_P^2} \cdot Z \tag{A9}$$

with μ_Z and k_P indicating the specific growth rate and the half saturation constant for grazing, respectively. Reported values for the half-saturation constant k_P span more than two orders of magnitude (Hansen et al., 1997) depending e.g. on species, age, nutritional state, or location. Therefore, the value of k_P has been determined in the calibration study. Compared to values compiled by Hirst and Bunker (2003) (e.g. 0.34 µmol P× l^{-1} for adult *Calanus* spp.) the value of 0.75 µmol P× l^{-1} is rather high. The possible reason for the overestimation of k_P in the model is the lack of a mortality term in the zooplankton growth equation Eq. A9, i.e. slower zooplankton growth implicitly accounts for the missing mortality term.

A4 Initial conditions and forcing

The surface PAR I_0 is regarded spatially uniform. Turbidity is a relative quantity that can be related to the diffuse light attenuation coefficient k_Z. This relationship is, however, variable and should be ideally established empirically (Davies-Colley and Smith, 2001). Here, it is estimated as

$$k_Z = a \cdot Tb + b \tag{A10}$$

with the parameters a=0.15 $\mathrm{m}^{-1} \times \mathrm{FTU}^{-1}$ and b=0.05 m^{-1}.
We assume that the initial value for the zooplankton concentration is a fraction r_Z of phytoplankton biomass P at the time $t_0 - \tau_Z$

$$Z(t_0,x_0) = \max(Z_{\min}, P(t_0 - \tau_Z, x_0) \cdot r_Z) \tag{A11}$$

where $Z_{\min}$ and τ_Z are the minimum zooplankton biomass and time lag for zooplankton, respectively. $Z_{\min}$ was determined to be 0.0075 µmol P× l^{-1} in the calibration study.

Acknowledgements. We thank F. Schroeder and W. Petersen for providing FerryBox data, J. Staneva for the hydrodynamic data from GETM and G. Flöser for the irradiance data from the GKSS measurement pile. We are grateful to D. Johns, Sir Alister Hardy Foundation for Ocean Science, for zooplankton data from the Continuous Plankton Recorder Survey. We thank two anonymous referees for valuable comments that helped to significantly improve the manuscript.

Edited by: A. Boetius

References

Ainsworth, C.: Oceanography: FerryBoxes Begin to Make Waves, Science, 322, 1627, 2008.

Beddig, S., Brockmann, U., Dannecker, W., Körner, D., Pohlmann, T., Puls, W., Radach, G., Rebers, A., Rick, H. J., Schatzmann, M., et al.: Nitrogen fluxes in the German Bight, Mar. Pollut. Bull., 34, 382–394, 1997.

Behrenfeld, M. J. and Falkowski, P. G.: Photosynthetic rates derived from satellite-based chlorophyll concentration, Limnol. Oceanogr., 42, 1–20, 1997.

Behrenfeld, M. J., Boss, E., Siegel, D. A., and Shea, D. M.: Carbon-based ocean productivity and phytoplankton physiology from space, Global Biogeochem. Cy., 19, doi:10.1029/2004GB002299, 2005.

Brandt, G., Wehrmann, A., and Wirtz, K.: Rapid invasion of *Crassostrea gigas* into the German Wadden Sea dominated by larval supply, J. Sea Res., 59, 279–296, 2008.

Cadée, G. C. and Hegeman, J.: Phytoplankton in the Marsdiep at the end of the 20th century; 30 years monitoring biomass, primary production, and Phaeocystis blooms, J. Sea Res., 48, 97–110, 2002.

Cloern, J. E.: An empirical model of the phytoplankton chlorophyll: Carbon ratio – the conversion factor between productivity and growth rate, Limnol. Oceanogr., 40, 1313–1321, 1995.

Cloern, J. E.: Phytoplankton bloom dynamics in coastal ecosystems: A review with some general lessons from sustained investigation of San Francisco Bay, California, Rev. Geophys., 34, 127–168, 1996.

Conover, R. J.: Assimilation of organic matter by zooplankton, Limnol. Oceanogr., 11, 338–345, 1966.

Davies-Colley, R. J. and Smith, D. G.: Turbidity, suspended sediment, and water clarity: A review, J. Am. Water. Resour. As., 37, 1085–1101, 2001.

Devlin, M. J., Barry, J., Mills, D. K., Gowen, R. J., Foden, J., Sivyer, D., and Tett, P.: Relationships between suspended particulate material, light attenuation and Secchi depth in UK marine waters, Estuar., Coast. and Shelf Sci., 79, 429–439, 2008.

Ebenhöh, W., Baretta-Bekker, J. G., and Baretta, J. W.: The primary production model in the ecosystem model ERSEM II, J. Sea Res., 38, 173–192, 1997.

Edwards, A. M. and Brindley, J.: Oscillatory behaviour in a three-component plankton population model, Dynam. Stabil. Syst., 11, 347–370, 1996.

Elser, J., Sterner, R., Galford, A., Chrzanowski, T., Findlay, D., Mills, K., Paterson, M., Stainton, M., and Schindler, D.: Pelagic C: N: P stoichiometry in a eutrophied lake: responses to a whole-lake food-web manipulation, Ecosystems, 3, 293–307, 2000.

Faure, V., Pinazo, C., Torréton, J. P., and Douillet, P.: Relevance of various formulations of phytoplankton chlorophyll *a*: carbon ratio in a 3D marine ecosystem model, C. R. Biologies, 329, 813–822, 2006.

Furnas, M. J.: In situ growth rates of marine phytoplankton: approaches to measurement, community and species growth rates, J. Plankton Res., 12, 1117–1151, 1990.

Geider, R. J.: Light and temperature depenence of the carbon to chlorophyll *a* ratio in microalgae and cyanobacteria: implications for physiology and growth of phytoplankton, New Phytol., 106, 1–34, 1987.

Geider, R. J., MacIntyre, H. L., and Kana, T. M.: A dynamic regulatory model of phytoplanktonic acclimation to light, nutrients, and temperature, Limnol. Oceanogr., 43, 679–694, 1998.

Gentleman, W., Leising, A., Frost, B., Strom, S., and Murray, J.: Functional responses for zooplankton feeding on multiple resources: a review of assumptions and biological dynamics, Deep-Sea Res. Pt. II, 50, 2847–2875, 2003.

Gismervik, I.: Stoichiometry of some marine planktonic crustaceans, J. Plankton Res., 19, 279–285, 1997.

Greve, W., Reiners, F., Nast, J., and Hoffmann, S.: Helgoland Roads meso- and macrozooplankton time-series 1974 to 2004: lessons from 30 years of single spot, high frequency sampling at the only off-shore island of the North Sea, Helgol. Mar. Res., 58, 274–288, 2004.

Halsband-Lenk, C., Nival, S., Carlotti, F., and Hirche, H.: Seasonal cycles of egg production of two planktonic copepods, *Centropages typicus* and *Temora stylifera*, in the north-western Mediterranean Sea, J. Plankton Res., 23, 597–609, 2001.

Hansen, P. J., Bjornsen, P. K., and Hansen, B. W.: Zooplankton grazing and growth: Scaling within the $2-2000\,\mu m$ body size range, Limnol. Oceanogr., 42, 687–704, 1997.

Hecky, R. E. and Kilham, P.: Nutrient limitation of phytoplankton in freshwater and marine environments: A review of recent evidence on the effects of enrichment., Limnol. Oceanogr., 33, 796–822, 1988.

Hirst, A. G. and Bunker, A. J.: Growth of marine planktonic copepods: global rates and patterns in relation to chlorophyll *a*, temperature, and body weight, Limnol. Oceanogr., 48, 1988–2010, 2003.

Iriarte, A. and Purdie, D. A.: Factors controlling the timing of major spring bloom events in an UK south coast estuary, Estuar., Coast. and Shelf Sci., 61, 679–690, 2004.

Irigoien, X., Flynn, K. J., and Harris, R. P.: Phytoplankton blooms: a "loophole" in microzooplankton grazing impact?, J. Plankton Res., 27, 313–321, 2005.

Joint, I. and Pomroy, A.: Phytoplankton biomass and production in the southern North Sea, Mar. Ecol. Prog. Ser., 99, 169–169, 1993.

Klausmeier, C., Litchman, E., and Levin, S.: Phytoplankton growth and stoichiometry under multiple nutrient limitation, Limnol. Oceanogr., 49, 1463–1470, 2004.

Kuipers, B. R. and van Noort, G. J.: Towards a natural Wadden Sea?, J. Sea Res., 60, 44–53, 2008.

Lacroix, G., Ruddick, K., Park, Y., Gypens, N., and Lancelot, C.: Validation of the 3D biogeochemical model MIRO&CO with field nutrient and phytoplankton data and MERIS-derived surface chlorophyll *a* images, J. Marine Sys., 64, 66–88, 2007.

Levin, S.: The problem of pattern and scale in ecology: the Robert

H. MacArthur award lecture, Ecology, 73, 1943–1967, 1992.
Llewellyn, C. A., Fishwick, J. R., and Blackford, J.: Phytoplankton community assemblage in the English Channel: a comparison using chlorophyll a derived from HPLC-CHEMTAX and carbon derived from microscopy cell counts, J. Plankton Res., 27, 103–119, 2005.
Loebl, M. and Beusekom, J. E. E. V.: Seasonality of microzooplankton grazing in the northern Wadden Sea, J. Sea Res., 59, 203–216, 2008.
Loebl, M., Colijn, F., van Beusekom, J. E. E., Baretta-Bekker, J. G., Lancelot, C., Philippart, C. J. M., Rousseau, V., and Wiltshire, K. H.: Recent patterns in potential phytoplankton limitation along the Northwest European continental coast, J. Sea Res., 61, 34–43, submitted, 2010.
Lucas, L., Koseff, J., Cloern, J., Monismith, S., and Thompson, J.: Processes governing phytoplankton blooms in estuaries. I: The local production-loss balance, Mar. Ecol. Prog. Ser., 187, 1–15, 1999a.
Lucas, L., Koseff, J., Monismith, S., Cloern, J., and Thompson, J.: Processes governing phytoplankton blooms in estuaries 2: The role of horizontal transport, Mar. Ecol. Prog. Ser., 187, 17–30, 1999b.
Lucas, L., Koseff, J., Monismith, S., and Thompson, J.: Shallow water processes govern system-wide phytoplankton bloom dynamics: A modeling study, J. Marine Sys., 75, 70–86, 2009.
Macedo, M. F., Duarte, P., Mendes, P., and Ferreira, J. G.: Annual variation of environmental variables, phytoplankton species composition and chotosynthetic carameters in a coastal lagoon, J. Plankton Res., 23, 719–732, 2001.
Martin, A.: Phytoplankton patchiness: the role of lateral stirring and mixing, Prog. Oceanogr., 57, 125–174, 2003.
May, C. L., Koseff, J. R., Lucas, L. V., Cloern, J. E., and Schoellhamer, D. H.: Effects of spatial and temporal variability of turbidity on phytoplankton blooms, Mar. Ecol. Prog. Ser., 254, 111–128, 2003.
Muylaert, K., Gonzales, R., Franck, M., Lionard, M., Van der Zee, C., Cattrijsse, A., Sabbe, K., Chou, L., and Vyverman, W.: Spatial variation in phytoplankton dynamics in the Belgian coastal zone of the North Sea studied by microscopy, HPLC-CHEMTAX and underway fluorescence recordings, J. Sea Res., 55, 253–265, 2006.
Nielsen, T. G.: Contribution of zooplankton grazing to the decline of a Ceratium bloom, Limnol. Oceanogr., 36, 1091–1106, 1991.
Pahlow, M.: Linking chlorophyll-nutrient dynamics to the Redfield N:C ratio with a model of optimal phytoplankton growth, Mar. Ecol. Prog. Ser., 287, 33–43, 2005.
Peperzak, L., Colijn, F., Gieskes, W. W. C., and Peeters, J. C. H.: Development of the diatom-Phaeocystis spring bloom in the Dutch coastal zone of the North Sea: the silicon depletion versus the daily irradiance threshold hypothesis, J. Plankton Res., 20, 517–537, 1998.
Petersen, W., Petschatnikov, M., Schroeder, F., and Colijn, F.: FerryBox systems for monitoring coastal waters, in: Building the European Capacity in Operational Oceanography: Proc. Third International Conference on EuroGOOS, Elsevier Oceanography Series Publication series, edited by: Dahlien, H., Flemming, N. C., Knittis, K., and Petersson, S. E., 19, 325–333, 2003.
Petersen, W., Wehde, H., Krasemann, H., Colijn, F., and Schroeder, F.: FerryBox and MERIS – Assessment of coastal and shelf sea ecosystems by combining in situ and remotely sensed data, Estuar. Coast. Shelf S., 77, 296–307, 2008.
Platt, T., Fuentes-Yaco, C., and Frank, K. T.: Marine ecology: spring algal bloom and larval fish survival, Nature, 423, 398–399, 2003.
Prins, T., Smaal, A., Pouwer, A., and Dankers, N.: Filtration and resuspension of particulate matter and phytoplankton on an intertidal mussel bed in the Oosterschelde estuary (SW Netherlands), Mar. Ecol. Prog. Ser., 142, 121–134, 1996.
Radach, G.: Ecosystem functioning in the German Bight under continental nutrient inputs by rivers, Estuaries Coasts, 15, 477–496, 1992.
Ragueneau, O., Quéguiner, B., and Tréguer, P.: Contrast in biological responses to tidally-induced vertical mixing for two macrotidal ecosystems of western Europe, Estuar. Coast. Shelf S., 42, 645–665, 1996.
Raven, J. A. and Geider, R. J.: Temperature and algal growth, New. Phytol., 110, 441–461, 1988.
Renz, J., Mengedoht, D., and Hirche, H.: Reproduction, growth and secondary production of *Pseudocalanus elongatus* Boeck (Copepoda, Calanoida) in the southern North Sea, J. Plankton Res., 30, 511–528, 2008.
Siegismund, F. and Schrum, C.: Decadal changes in the wind forcing over the North Sea, Climate Res., 18, 39–45, 2001.
Skogen, M. D. and Moll, A.: Importance of ocean circulation in ecological modeling: An example from the North Sea, J. Marine Sys., 57, 289–300, 2005.
Skogen, M. D., Söiland, H., and Svendson, E.: Effects of changing nutrient loads to the North Sea, J. Marine Sys., 46, 23–38, 2004.
Smetacek, V. and Cloern, J. E.: Oceans: On Phytoplankton Trends, Science, 319, 1346, 2008.
Soetaert, A. F. H. K. and Middelburg, J. J.: Present nitrogen and carbon dynamics in the Scheldt estuary using a novel 1-D model, Biogeosciences, 5, 981–1006, 2008, http://www.biogeosciences.net/5/981/2008/.
Sommer, U.: Biologische Meereskunde, Springer, 1998.
Sommer, U. and Lengfellner, K.: Climate change and the timing, magnitude, and composition of the phytoplankton spring bloom, Glob. Change Biolo., 14, 1199–1208, 2008.
Staneva, J., Stanev, E. V., Wolff, J. O., Badewien, T., Reuter, R., Flemming, B., Bartholomä, and Bolding, K.: Hydrodynamics and sediment dynamics in the German Bight. A focus on observations and numerical modelling in the East Frisian Sea, Cont. Shelf. Res., 29, 302–319, 2009.
Stelfox-Widdicombe, C. E., Archer, S. D., Burkill, P. H., and Stefels, J.: Microzooplankton grazing in Phaeocystis and diatom-dominated waters in the southern North Sea in spring, J. Sea Res., 51, 37–51, 2004.
Stips, A., Bolding, K., Pohlmann, T., and Burchard, H.: Simulating the temporal and spatial dynamics of the North Sea using the new model GETM (General Estuarine Transport Model), Ocean Dyn., 54, 266–283, 2004.
Taylor, A. H., Geider, R. J., and Gilbert, F. J. H.: Seasonal and latitudinal dependencies of phytoplankton carbon-to-chlorophyll *a* ratios: results of a modelling study, Mar. Ecol. Prog. Ser., 152, 51–66, 1997.
Tett, P., Heaney, S. I., and Droop, M. R.: The redfield ratio and phytoplankton growth rate., J. Mar. Biol. Assoc. U.K., 65, 487–504, 1985.

Thomas, A., Townsend, D., and Weatherbee, R.: Satellite-measured phytoplankton variability in the Gulf of Maine, Cont. Shelf. Res., 23, 971–989, 2003.

Tian, T., Merico, A., Su, J., Staneva, J., Wiltshire, K., and Wirtz, K.: Importance of resuspended sediment dynamics for the phytoplankton spring bloom in a coastal marine ecosystem, J. Sea Res., 62, 214–228, 2009.

Tilzer, M. M.: The importance of fractional light absorption by photosynthetic pigments for phytoplankton productivity in Lake Constance., Limnol. Oceanogr., 28, 833–846, 1983.

Townsend, D., Cammen, L., Holligan, P., Campbell, D., and Pettigrew, N.: Causes and consequences of variability in the timing of spring phytoplankton blooms, Deep-Sea Res. Pt. I, 41, 747–765, 1994.

van der Zee, C. and Chou, L.: Seasonal cycling of phosphorus in the Southern Bight of the North Sea, Biogeosciences, 2, 27–42, 2005,
http://www.biogeosciences.net/2/27/2005/.

Verity, P. G.: Measurement and simulation of prey uptake by marine planktonic ciliates fed plastidic and aplastidic nanoplankton., Limnol. Oceanogr., 36, 729–750, 1991.

Weston, K., Greenwood, N., Fernand, L., Pearce, D. J., and Sivyer, D. B.: Environmental controls on phytoplankton community composition in the Thames plume, UK, J. Sea Res., 60, 262–270, 2008.

Wiltshire, K. H. and Manly, B. F. J.: The warming trend at Helgoland Roads, North Sea: phytoplankton response, Helgol. Mar. Res., 58, 269–273, 2004.

Wiltshire, K. H., Malzahn, A. M., Wirtz, K. W., Greve, W., Janisch, S., Mangelsdorf, P., Manly, B. F. J., and Boersma, M.: Resilience of North Sea phytoplankton spring bloom dynamics: An analysis of long-term data at Helgoland Roads, Limnol. Oceanogr., 53, 1294–1302, 2008.

Wirtz, K. W. and Eckhardt, B.: Effective variables in ecosystem models with an application to phytoplankton succession, Ecol. Modell., 92, 33–53, 1996.

Woods, J., Perilli, A., and Barkmann, W.: Stability and predictability of a virtual plankton ecosystem created with an individual-based model, Prog. Oceanogr., 2005.